Title	Interaction between terrestrial plasma sheet electrons and the lunar surface: SELENE (Kaguya) observations
Author(s)	Harada, Yuki; Machida, Shinobu; Saito, Yoshifumi; Yokota, Shoichiro; Asamura, Kazushi; Nishino, Masaki N.; Tanaka, Takaaki; Tsunakawa, Hideo; Shibuya, Hidetoshi; Takahashi, Futoshi; Matsushima, Masaki; Shimizu, Hisayoshi
Citation	Geophysical Research Letters (2010), 37(19)
Issue Date	2010-10
URL	http://hdl.handle.net/2433/131758
Right	©2010. American Geophysical Union.
Type	Journal Article
Textversion	author

GEOPHYSICAL RESEARCH LETTERS, VOL. ???, XXXX, DOI:10.1029/,

Interaction between terrestrial plasma sheet electrons and the lunar surface: SELENE (Kaguya) observations

Yuki Harada,[1] Shinobu Machida,[1] Yoshifumi Saito,[2] Shoichiro Yokota,[2] Kazushi Asamura,[2] Masaki N. Nishino,[2] Takaaki Tanaka,[2] Hideo Tsunakawa,[3] Hidetoshi Shibuya,[4] Futoshi Takahashi,[3] Masaki Matsushima,[3] and Hisayoshi Shimizu[5]

Y. Harada and S. Machida, Department of Geophysics, Kyoto University, Oiwake-machi, Sakyo-ku, Kyoto 606-8502, Japan. (haraday@kugi.kyoto-u.ac.jp)

K. Asamura, M. N. Nishino, Y. Saito, T. Tanaka and S. Yokota, Institute of Space and Astronautical Science, Japan Aerospace Exploration Agency, 3-1-1 Yoshinodai, Chuo-ku, Sagamihara 229-8510, Japan.

M. Matsushima, F. Takahashi and H. Tsunakawa, Department of Earth and Planetary Sciences, Tokyo Institute of Technology, 2-12-1 Ookayama, Tokyo 152-8551, Japan.

H. Shibuya, Department of Earth and Environmental Sciences, Kumamoto University, Kumamoto 860-8555, Japan.

H. Shimizu, Earthquake Research Institute, University of Tokyo, 1-1-1 Yayoi, Tokyo 113-0032, Japan.

[1]Department of Geophysics, Kyoto

Analysis of the data obtained by SELENE (Kaguya) revealed a partial loss in the electron velocity distribution function due to the "gyro-loss effect", namely gyrating electrons being absorbed by the lunar surface. The Moon enters the Earth's magnetosphere for a few days around full moon, where plasma conditions are significantly different from those in the solar wind. When the magnetic field is locally parallel to the lunar surface, relatively high-energy electrons in the terrestrial plasma sheet with Larmor radii greater than SELENE's orbital height strike the lunar surface and are absorbed before they can be detected. This phenomenon can be observed as an empty region in

University, Kyoto, Japan.

[2]Institute of Space and Astronautical Science, Japan Aerospace Exploration Agency, Sagamihara, Japan.

[3]Department of Earth and Planetary Sciences, Tokyo Institute of Technology, Tokyo, Japan.

[4]Department of Earth and Environmental Sciences, Kumamoto University, Kumamoto, Japan.

[5]Earthquake Research Institute, University of Tokyo, Tokyo, Japan.

the electron distribution function, which is initially isotropic in the plasma sheet, resulting in a non-gyrotropic distribution. We observed the expected characteristic electron distributions, as well as an empty region that was consistent with the presence of a relatively strong electric field (~ 10 mV/m) around the Moon when it is in the plasma sheet.

1. Introduction

The Moon does not possess a global magnetic field or a thick atmosphere [*Ness et al.*, 1967]. Therefore, the plasma around the Moon is ideal for investigating the interaction of charged particles with large solid bodies. The Moon enters the Earth's magnetosphere for a few days around full moon. The plasma in the magnetosphere has different properties from the solar wind, including different densities and energies, and it interacts directly with the lunar surface [*Rich et al.*, 1973; *Schubert et al.*, 1974].

The first measurements of the lunar plasma environment were made by Explorer 35 in the solar wind and the Earth's magnetosphere [*Lyon et al.*, 1967; *Nishida and Lyon*, 1972]. Apollo 15 and 16 subsatellites observed electrons reflected from lunar crustal magnetic fields and measured the surface magnetic field intensity by electron reflectometry [*Howe et al.*, 1974]. Without crustal magnetic fields, almost all the electrons that strike the lunar surface will be absorbed, although some backscattering as well as secondary electron emission exist [*Halekas et al.*, 2009]. Electrons adiabatically reflected due to the magnetic mirror effect produce a loss cone in the upgoing electron velocity distribution function (VDF). The surface magnetic field B_{surf} is inferred by measuring both the magnetic field B_{sc} and the electron loss cone (cutoff pitch angle α_c) at the spacecraft, using the relationship $B_{\mathrm{surf}} = B_{\mathrm{sc}}/\sin^2\alpha_c$. This method was also used to produce a global map of the lunar crustal magnetic fields by Lunar Prospector [*Halekas et al.*, 2001; *Mitchell et al.*, 2008], Additionally these observations revealed energy-dependent loss cones, indicating reflection by both electric and magnetic fields [*Halekas et al.*, 2002]. The electrostatic potential of the lunar surface varies in sunlight and shadow, and depends on the ambient plasma conditions, which vary depending on whether the Moon is in the solar wind, terrestrial magnetotail lobe, or the plasma sheet [*Halekas et al.*, 2008]. The large range of lunar surface potentials implies that the electric field around the Moon is highly variable.

Electron reflectometry can be used when the magnetic field line passing through the observer intersects the Moon, because electrons travel along magnetic field lines. By analyzing the data obtained by SELENE (Kaguya), we found an interesting phenomenon concerning electrons in the terrestrial plasma sheet when the magnetic field line is parallel to the lunar surface; gyrating electrons are absorbed by the lunar surface, and a partial loss appears in the electron VDF due to this "gyro-loss effect". In this paper, we refer to "empty regions" when we are describing features in observations, while "forbidden regions" when we are describing theoretical predictions.

2. Instrumentation

SELENE is a Japanese lunar orbiter that was launched on 14 September 2007 and entered a circular lunar polar orbit with an altitude of 100 km. Since SELENE is a three-axis stabilized spacecraft, one of its panels always faces the lunar surface. Magnetic field and plasma measurements were conducted by the MAgnetic field and Plasma experiment (MAP) onboard SELENE, which consists of the Lunar MAGnetometer (LMAG) and the Plasma energy Angle and Composition Experiment (PACE). LMAG is a triaxial fluxgate magnetometer used to observe the magnetic field around the Moon with a sampling frequency of 32 Hz and a resolution of 0.1 nT [*Shimizu et al.*, 2008; *Takahashi et al.*, 2009; *Tsunakawa et al.*, 2010]. PACE was designed to perform three-dimensional plasma measurements around the Moon [*Saito et al.*, 2008]. It consists of four sensors:

two electron spectrum analyzers (ESA-S1 and ESA-S2), an ion mass analyzer (IMA), and an ion energy analyzer (IEA). ESA-S1 and ESA-S2 measure the distribution function of low-energy electrons with energies below 16 keV, while IMA and IEA measure the distribution function of low-energy ions with energies below 29 keV/q. Figure 1 shows the satellite coordinates of SELENE. ESA-S1 and IMA are installed on the +Z panel (looking down toward the lunar surface), while ESA-S2 and IEA are on the -Z panel (looking away from the lunar surface). Each sensor has a hemispherical field of view.

3. Theoretical Predictions

Electrons gyrate around magnetic field lines with a Larmor radii given by $r_L = m_e v_\perp / eB$, where m_e is the electron mass, $v_\perp$ is the electron velocity component perpendicular to the magnetic field, e is the elementary charge, and B is the magnetic field intensity. Although most electrons in the Earth's magnetosphere gyrate with a smaller Larmor radii than the orbital height H (nominal value: 20–100 km) of SELENE, some electrons in the plasma sheet have Larmor radii greater than or equal to H (e.g., a 1 keV electron has a Larmor radius of 107 km in a 1 nT magnetic field). When the magnetic field is parallel to the lunar surface, these relatively high-energy electrons strike the lunar surface and are absorbed (Figure 2a). This can be observed as an empty region in the electron VDF, which is isotropic in the terrestrial plasma sheet [*Machida et al.*, 1994].

Consider an electron entering the sensors with a perpendicular velocity component $v_\perp$ and a gyrophase ψ, as shown in Figure 2b. Here, the lunar surface is assumed to be planar since H is much smaller than the lunar radius, 1738 km. From the geometry, the critical

Larmor radius r_c is given by

$$r_c = \frac{H}{1 - \cos\psi}. \tag{1}$$

Electrons with $r_L \geq r_c$ are absorbed by the surface and therefore cannot be observed. At higher energies, more electrons will be absorbed, enlarging the empty region in the electron VDF. When $\psi = 180°$, r_c takes a minimum value $H/2$ and the cut-off energy of electrons will be a minimum. On the other hand, r_c is infinite when $\psi = 0°$ and no electrons will be cut off.

In the case of an electric field component perpendicular to the magnetic field as indicated in Figure 2c, electrons will drift toward the lunar surface. If we take the guiding center rest frame (quantities are indicated by '), the lunar surface effectively approaches the spacecraft with the $\mathbf{E} \times \mathbf{B}$ drift velocity $v_{E\times B}$. Since the time in which an electron gyrates from a point nearest the lunar surface to SELENE (the red solid arc in Figure 2c) $t_{\psi'}$ is described as $t_{\psi'} = r'_L\psi'/v'_\perp = m_e\psi'/eB$ (with ψ' in radians), the critical Larmor radius will be modified as follows:

$$r'_c = \frac{H'}{1 - \cos\psi'} = \frac{H + v_{E\times B}t_{\psi'}}{1 - \cos\psi'} = \frac{H + \frac{E_\perp}{B}\frac{m_e}{eB}\psi'}{1 - \cos\psi'}. \tag{2}$$

Electrons that satisfy $r'_L \geq r'_c$ strike the lunar surface and are absorbed. If $E_\perp > 0$, the forbidden region will be smaller than the previous case because $r'_c > r_c$.

4. Observations

Table 1 shows the location of the Moon and SELENE, as well as the ambient plasma conditions for two events discussed below. Figure 3 shows an electron angular distribution observed during Event 1. The red lines show the forbidden regions derived from equation

(1). At this time, B was 5.4 nT and relatively high-energy electrons ($\geq$ 1 keV) were detected. Therefore, the Moon was thought to be located in the plasma sheet or in the plasma sheet boundary layer, and SELENE was located on the dayside of the Moon at (Lat. 33°N, Lon. 0°) where strong magnetic anomalies do not exist. During this time interval, the magnetic field was nearly stable and parallel to the lunar surface and it had an azimuthal angle (in the satellite coordinates X-Y plane) of about 222°. Empty regions in the electron distribution appeared at an azimuthal angle of around 312°, where $\psi = 180°$ and r_c is a minimum. As expected, high-energy empty regions were larger than low-energy empty regions. These empty regions seem to correspond to theoretically derived forbidden regions.

Figure 4 shows another example observed during Event 2, when SELENE was located at (Lat. 28°S, Lon. 92°W) where strong magnetic anomalies do not exist. At this time, the Moon was in the central plasma sheet. The magnetic field line was nearly stable and parallel to the lunar surface (although it was slightly inclined in this example) and it had an azimuthal angle (in the satellite coordinates X-Y plane) of about 238°. Empty regions also appeared around 328° in Figure 4, but the forbidden regions derived from equation (1) (solid red lines) are larger than the observed empty regions. By assuming that the perpendicular electric field is 10 mV/m in equation (2), we can fit the forbidden regions (broken red lines).

5. Discussion

By analyzing the data obtained by SELENE, we discovered characteristic electron VDFs produced by the interaction between terrestrial plasma sheet electrons and the lunar surface. We compared theoretically derived forbidden regions with the observed empty regions in electron VDFs and found that such forbidden regions do exist. Interestingly, these electron VDFs are asymmetric relative to the magnetic field line; in other words, they are "non-gyrotropic". Such non-gyrotropic VDFs are very rare in space plasmas, especially for electrons in a steady state. However, these VDFs commonly exist at low altitudes around the Moon. We note that field aligned upward-going electron beams and energy-dependent loss cones observed when the magnetic field line intersects the lunar surface [*Halekas et al.*, 2002] are "gyrotropic" VDFs (symmetric with respect to the magnetic field line).

The empty regions in Figure 4 are more consistent with the forbidden regions in the presence of a perpendicular electric field than those when no perpendicular electric field is present. This finding suggests that a relatively strong electric field ($\sim$ 10 mV/m) exists around the Moon in the plasma sheet, although other explanations are also possible. For example, the plasma can be diffused in phase space to form a smaller empty region due to scattering by unstable waves [*Kennel and Petschek*, 1966].

An electric field of 10 mV/m is quite strong in the Earth's magnetotail near lunar orbit (*McCoy et al.* [1975] reported typical value of 0.15 mV/m and up to 2 mV/m). When $B = 2.2$ nT and $E_\perp = 10$ mV/m, we can get $v_{E\times B} = 4.5 \times 10^3$ km/s. However, the bulk flow obtained from the ion observation in Event 2 was 410 km/s (Table 1). Therefore, ions did not execute $\mathbf{E} \times \mathbf{B}$ drift and the scale length of the region characterized by the strong electric field was less than the diameter of the ion gyromotion (i.e. twice of the ion Larmor radius).

In Event 2, SELENE was located near the terminator of the Moon (solar zenith angle 106°) and assumed $E_\perp$ is $(-6.3, -2.0, 7.5)$ mV/m in SSE coordinates. This electric field has $-x$ component, which is directed from the sunlit side to the night side. Therefore, the potential difference between the two sides (the electrostatic potential is higher in the sunlit side than the night side due to photoelectron emission) may generate this electric field. However, this idea has to be considered carefully since a Debye length around the Moon (< 1 km) is much smaller than SELENE's orbital height H and the surface potential can be shielded within a few Debye lengths. [*Farrell et al.*, 2007].

6. Conclusions

A partial loss in the electron VDF due to the "gyro-loss effect" was discovered. Electron VDFs produced by this effect are "non-gyrotropic" VDFs which are very rare in space plasmas. The phenomena discussed above are not limited to the case of terrestrial electrons and the Moon, but general and fundamental processes when a plasma interacts with a solid surface. The electron VDFs suggest a relatively strong electric field is sometimes present in the near-lunar plasma environment. This study can be used as a technique to measure electric fields in the vicinity of the Moon.

Acknowledgments. The authors wish to express their sincere thanks to the team members of MAP-PACE and MAP-LMAG for their great support in processing and analyzing the MAP data. The authors also wish to express their gratitude to the system members of the SELENE project. SELENE-MAP-PACE sensors were manufactured by Mitaka Kohki Co. Ltd., Meisei Elec. Co., Hamamatsu Photonics K.K., and Kyocera Co.

References

Farrell, W. M., T. J. Stubbs, R. R. Vondrak, G. T. Delory, and J. S. Halekas (2007), Complex electric fields near the lunar terminator: The near-surface wake and accelerated dust, *Geophys. Res. Lett.*, *34*, L14201.

Halekas, J. S., D. L. Mitchell, R. P. Lin, S. Frey, L. L. Hood, M. H. Acuña, and A. B. Binder (2001), Mapping of crustal magnetic anomalies on the lunar near side by the lunar prospector electron reflectometer, *J. Geophys. Res.*, *106*, 27,841–27,852.

Halekas, J. S., D. L. Mitchell, R. P. Lin, L. L. Hood, M. H. Acuña, and A. B. Binder (2002), Evidence for negative charging of the lunar surface in shadow, *Geophys. Res. Lett.*, *29*, 1435.

Halekas, J. S., G. T. Delory, R. P. Lin, T. J. Stubbs, and W. M. Farrell (2008), Lunar prospector observations of the electrostatic potential of the lunar surface and its response to incident currents, *J. Geophys. Res.*, *113*, A09102.

Halekas, J. S., G. T. Delory, R. P. Lin, T. J. Stubbs, and W. M. Farrell (2009), Lunar prospector measurements of secondary electron emission from lunar regolith, *Planet. Space Sci.*, *57*, 78–82.

Howe, H. C., R. P. Lin, R. E. McGuire, and K. A. Anderson (1974), Energetic electron scattering from the lunar remanent magnetic field, *Geophys. Res. Lett.*, *1*, 101–104.

Kennel, C. F., and H. E. Petschek (1966), Limit on stably trapped particle fluxes, *J. Geophys. Res.*, *71*, 1–28.

Lyon, E. F., H. S. Bridge, and J. H. Binsack (1967), Explorer 35 plasma measurements in the vicinity of the moon, *J. Geophys. Res.*, *72*, 6113–6117.

Machida, S., T. Mukai, Y. Saito, T. Obara, T. Yamamoto, A. Nishida, M. Hirahara, T. Terasawa, and S. Kokubun (1994), GEOTAIL low energy particle and magnetic field observations of a plasmoid at $x_{GSM} = -142 r_E$, *Geophys. Res. Lett.*, *21*, 2995–2998.

McCoy, J. E., R. P. Lin, R. E. McGuire, L. M. Chase, and K. A. Anderson (1975), Magnetotail electric fields observed from lunar orbit, *J. Geophys. Res.*, *80*, 3217–3224.

Mitchell, D. L., J. S. Halekas, R. P. Lin, S. Frey, L. L. Hood, M. H. Acuña, and A. Binder (2008), Global mapping of lunar crustal magnetic fields by lunar prospector, *Icarus*, *194*, 401–409.

Ness, N. F., K. W. Behannon, C. S. Scearce, and S. C. Cantara (1967), Early results from the magnetic field experiment on lunar explorer 35, *J. Geophys. Res.*, *72*, 5769–5778.

Nishida, A., and E. F. Lyon (1972), Plasma sheet at lunar distance: Structure and solar-wind dependence, *J. Geophys. Res.*, *77*, 4086–4099.

Rich, F. J., D. L. Reasoner, and W. J. Burke (1973), Plasma Sheet at Lunar Distance: Characteristics and Interactions with the Lunar Surface, *J. Geophys. Res.*, *78*(34), 8097–8112.

Saito, Y., et al. (2008), Low-energy charged particle measurement by MAP-PACE onboard SELENE, *Earth Planets Space*, *60*, 375–385.

Schubert, G., B. R. Lichtenstein, C. T. Russell, P. J. C. Jr., B. F. Smith, D. S. Colburn, and C. P. Sonett (1974), Lunar dayside plasma sheet depletion: Inference from magnetic observations, *Geophys. Res. Lett.*, *1*, 97–100.

Shimizu, H., F. Takahashi, N. Horii, A. Matsuoka, M. Matsushima, H. Shibuya, and H. Tsunakawa (2008), Ground calibration of the high-sensitivity SELENE lunar mag-

Table 1. Moon and SELENE locations and ambient plasma conditions for two events.

	Event 1	Event 2
Time period	2009/05/06/22:22:11-22:22:27	2008/01/21/15:00:23-15:01:11
Moon location in GSE coordinates	(-53, 27, -5)R_E	(-57, 12, 3)R_E
SELENE location		
- Orbital height	51 km	98 km
- Latitude and longitude in selenographic coordinates	(33°N, 0°)	(28°S, 92°W)
- Solar zenith angle	43°	106°
Magnetic field intensity	5.4 nT	2.2 nT
Density	0.15 cm^{-3}	0.07 cm^{-3}
Ion temperature	476 eV	1.86 keV
Electron temperature	361 eV	435 eV
Bulk flow	–	410 km/s

netometer LMAG, *Earth Planets Space*, *60*, 353–363.

Takahashi, F., H. Shimizu, M. Matsushima, H. Shibuya, A. Matsuoka, S. Nakazawa, Y. Iijima, H. Otake, and H. Tsunakawa (2009), In-orbit calibration of the lunar magnetometer onboard SELENE (KAGUYA), *Earth Planets Space*, *61*, 1269–1274.

Tsunakawa, H., H. Shibuya, F. Takahashi, H. Shimizu, M. Matsushima, A. Matsuoka, S. Nakazawa, H. Otake, and Y. Iijima (2010), Lunar magnetic field observation and initial global mapping of lunar magnetic anomalies by MAP-LMAG onboard SELENE (Kaguya), *Space Sci. Rev.*, doi:10.1007/s11214-010-9652-0.

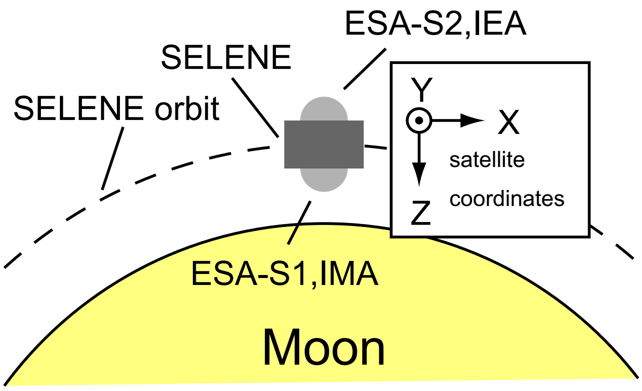

Figure 1. Satellite coordinates of SELENE. +Z is directed toward the lunar surface; +X or -X is the direction of travel; and Y completes the orthogonal set.

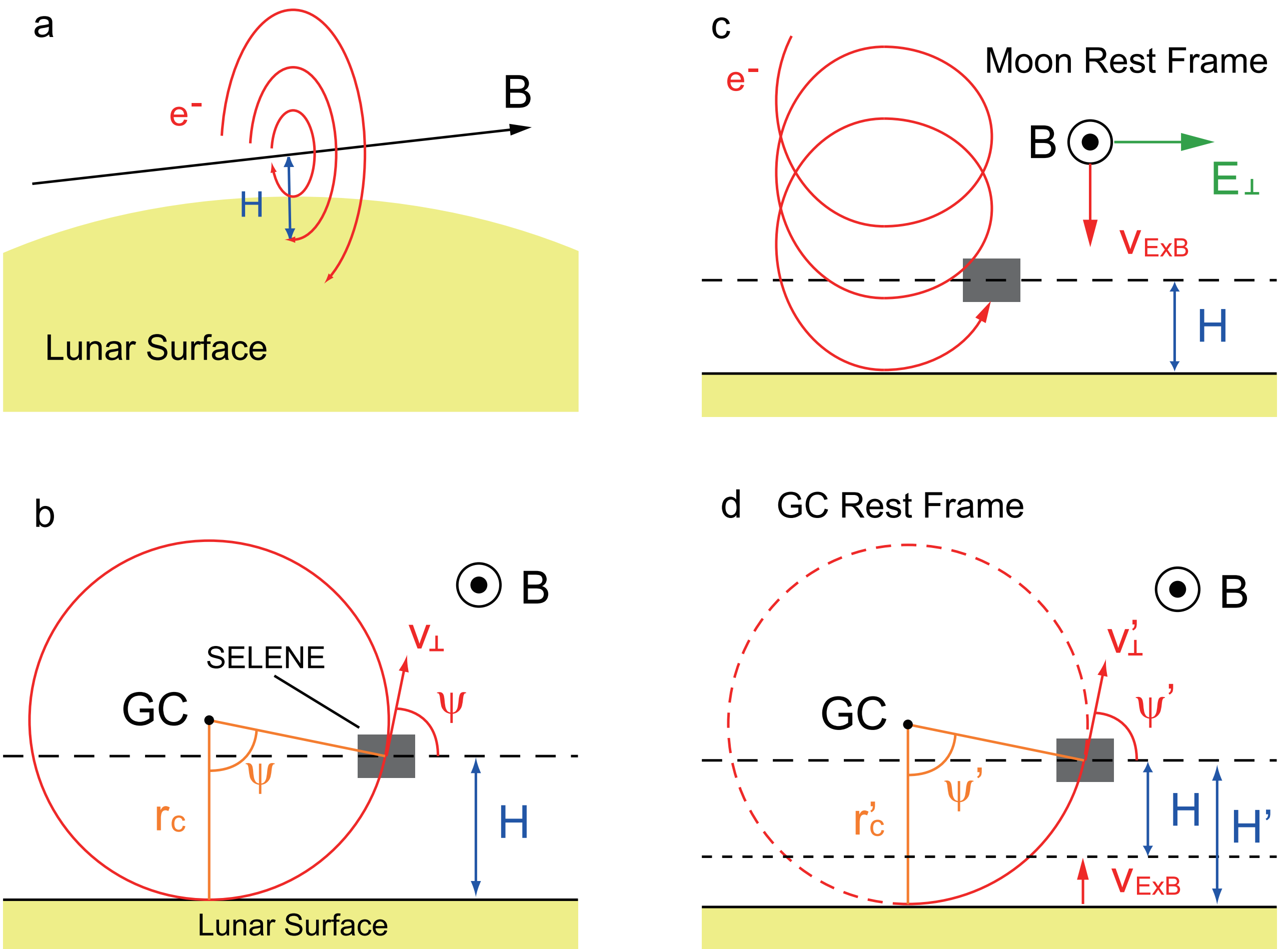

Figure 2. Schematic illustration of (a) interaction between electrons and the lunar surface, (b) the critical Larmor radius r_c, gyrophase ψ, perpendicular velocity $v_\perp$, and SELENE's orbital height H, and the case of an electric field perpendicular to the magnetic field in (c) the Moon's rest frame and (d) in the guiding center (GC) rest frame. GC indicates the guiding center of the electron.

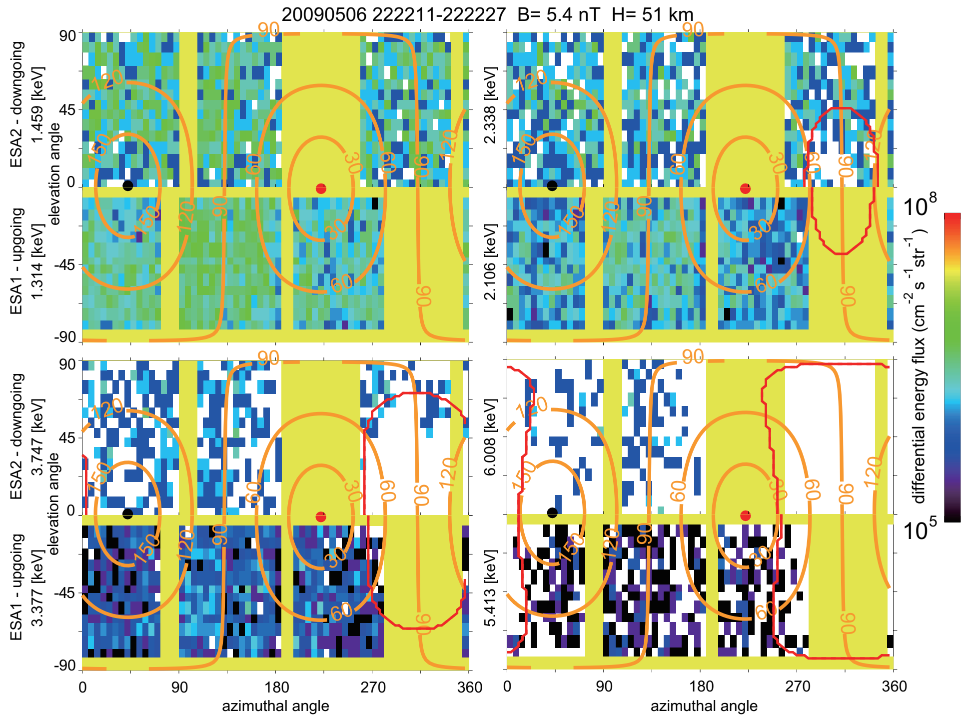

Figure 3. Electron angular distribution for different energies in satellite coordinates obtained during 22:22:11-22:22:27 UT (16 sec) on 6 May 2009, when the Moon was in the Earth's magnetotail and the magnetic field was nearly parallel to the lunar surface. The top left panel shows the distributions of electrons with energies of 1.459 (ESA-S2) and 1.314 (ESA-S1) keV, the top right panel shows those with energies of 2.338 (ESA-S2) and 2.106 (ESA-S1) keV. The bottom left panel shows the distributions of electrons with energies of 3.747 (ESA-S2) and 3.377 (ESA-S1) keV, and the bottom right panel shows those with energies of 6.008 (ESA-S2) and 5.413 (ESA-S1) keV. Angles with little or no sensitivity are indicated by yellow. Note that ESA-S1 and ESA-S2 have different sensitivities. The red and black circles respectively indicate the magnetic field direction and the opposite direction obtained from LMAG data. The orange contours indicate the pitch angles. The red lines indicate the theoretically derived forbidden regions assuming that there is no perpendicular electric field.

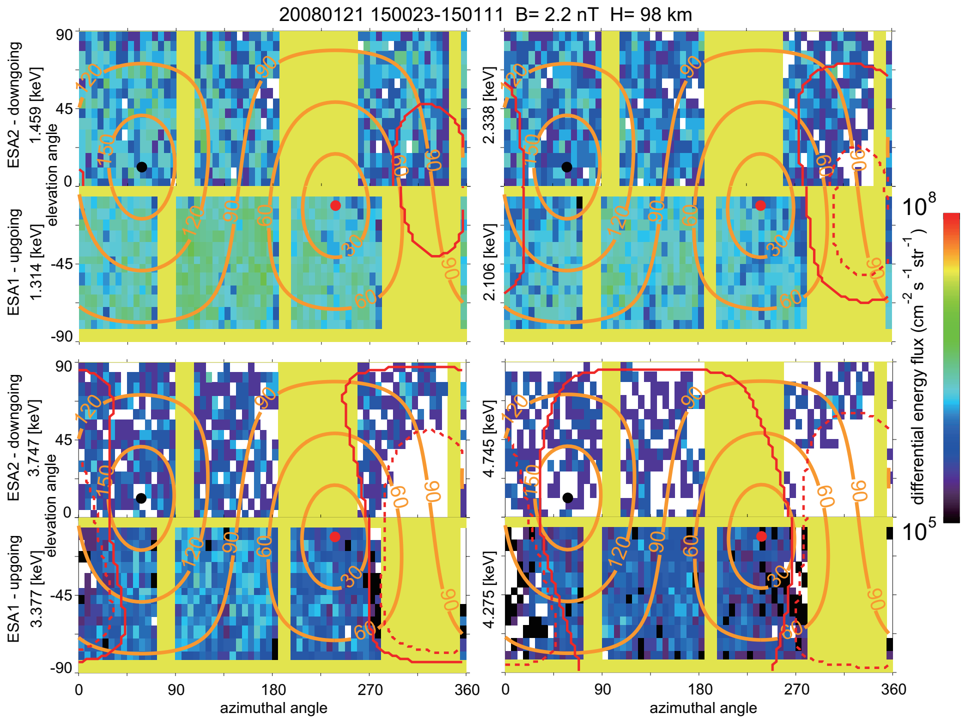

Figure 4. Electron angular distribution obtained during 15:00:23-15:01:11 UT (48 sec averaged) on 21 January 2008, in the same format as Figure 3. The broken red lines indicate the theoretically derived forbidden regions assuming a perpendicular electric field of 10 mV/m, whereas the solid red lines indicate regions with no electric field.